J Biomol NMR (2011) 49:195–206
DOI 10.1007/s10858-011-9490-8

ARTICLE

NMR-based metabolomics of mammalian cell and tissue cultures

Nelly Aranibar · Michael Borys · Nancy A. Mackin · Van Ly · Nicholas Abu-Absi · Susan Abu-Absi · Matthias Niemitz · Bernhard Schilling · Zheng Jian Li · Barry Brock · Reb J. Russell II · Adrienne Tymiak · Michael D. Reily

Received: 22 November 2010 / Accepted: 3 January 2011 / Published online: 4 March 2011

Abstract NMR spectroscopy was used to evaluate growth media and the cellular metabolome in two systems of interest to biomedical research. The first of these was a Chinese hamster ovary cell line engineered to express a recombinant protein. Here, NMR spectroscopy and a quantum mechanical total line shape analysis were utilized to quantify 30 metabolites such as amino acids, Krebs cycle intermediates, activated sugars, cofactors, and others in both media and cell extracts. The impact of bioreactor scale and addition of anti-apoptotic agents to the media on the extracellular and intracellular metabolome indicated changes in metabolic pathways of energy utilization. These results shed light into culture parameters that can be manipulated to optimize growth and protein production. Second, metabolomic analysis was performed on the superfusion media in a common model used for drug metabolism and toxicology studies, in vitro liver slices. In this study, it is demonstrated that two of the 48 standard media components, choline and histidine are depleted at a faster rate than many other nutrients. Augmenting the starting media with extra choline and histidine improves the long-term liver slice viability as measured by higher tissues levels of lactate dehydrogenase (LDH), glutathione and ATP, as well as lower LDH levels in the media at time points out to 94 h after initiation of incubation. In both models, media components and cellular metabolites are measured over time and correlated with currently accepted endpoint measures.

Keywords Metabolomics · NMR · Liver slice · CHO cell · Bioreactor · Bioprocess

M. Borys · N. A. Mackin · N. Abu-Absi · S. Abu-Absi · B. Schilling · Z. J. Li
Bristol-Myers Squibb Company, 6000 Thompson Road, Syracuse, NY 13057, USA

R. J. Russell II
Bristol-Myers Squibb Company, 311 Pennington-Rocky Hill Road, Pennington, NJ 08534, USA

M. Niemitz
PERCH Solutions Ltd., Hyrräkatu 3A1, 70500 Kuopio, Finland

N. Aranibar · V. Ly · B. Brock · A. Tymiak · M. D. Reily (✉)
Bristol-Myers Squibb Company, Route 206 and Province Line Road, Princeton, NJ 08540, USA
e-mail: michael.reily@bms.com

Introduction

Early work in the area of metabolomics (also known as metabonomics) was motivated to help understand the systems biology in human health (Pauling et al. 1971; Jellum et al. 1988; Adams et al. 1999), toxicology (Nicholson et al. 1999), and plant science (Sauter et al. 1991; Trethewey et al. 1999). In metabolomics, the objective is typically to measure as many small molecule components in a given matrix as possible, and use this information to understand the biology of the system under study. Numerous analytical tools have been applied to this endeavor, the bulk of which have focused on mass spectrometry and NMR spectroscopy (Robertson et al. 2007; Issaq et al. 2009). NMR has played a significant role in the development of this field because of its ability to quantify individual species in complex mixtures (Lindon 1999).

Important medical needs that are difficult to address with traditional small molecule drugs have fostered an increased interest in protein and nucleic acid-based therapeutics. These so-called "biologics" (especially proteins) are frequently manufactured through expression in genetically modified mammalian or bacterial cells. At later stages of

drug development, the cell culture vessels can reach capacities of 20,000 L, produce 100 kg of drug product and cost millions of dollars per run. With a fixed cost per culture, it is obvious that even a modest increase in yield (protein titer) represents a substantial reduction in the per-dose cost of the final drug product. Earlier in drug discovery, the importance of producing safe and efficacious medicines, both large and small, has led to the establishment of many in vitro testing models that provide early information on drug metabolism and toxicity. One of these models is the in vitro liver slice assay, where thin slices of liver are suspended in defined media and treated with drug. The slice and/or media are then analyzed over time to determine how the drug is either metabolized or what effects it has on the liver slice. These approaches, born of scientific, safety and cost incentives, have contributed to the development of novel applications of metabolomics in the area of analysis of cell cultures expressing protein therapeutics (Chong et al. 2009, 2010; Bradley et al. 2010; Chrysanthopoulos et al. 2010; Cuperlovic-Culf et al. 2010; Lim et al. 2010) and to a lesser extent mammalian tissue cultures (Gomez-Lechon et al. 2010; Seagle et al. 2008; Dunn et al. 2009).

In order to apply metabolomics to such systems, it must be possible to accurately quantify the small molecule endogenous metabolites produced by or utilized by the cells or tissues in culture. For prominent components and those that have peaks that are well separated from interfering peaks, simple integration normally does an adequate job of quantification. However, frequently one encounters situations where critical changes occur in low-level metabolites or in crowded regions of the NMR spectrum and achieving accurate quantitation can be a challenging in such circumstances. In the case of cell and tissue culture, this is further complicated because mammalian cells often require the presence of proteins in their media (e.g. fetal bovine serum) and produce proteins which are excreted into the supernatants. Such biomolecules produce broad signals detected in the NMR spectrum as the so-called 'protein envelope'. These broad background resonance signals make simple integration and 'bucketing' or 'binning' approaches impracticable or at least inaccurate. On the other hand, NMR methods used for reduction of broad lines such as T2 filtering depend on the correlation time and quantity of the proteins present which may not be the same across all samples. This confounding factor affects the accurate quantization of metabolites, which themselves, are following non-linear rates of change across the cell's life time.

In this work, we present metabolomics results on two systems of relevance to pharmaceutical research and development: the CHO cell expression system for protein therapeutic production and the rat liver slice model for assessing drug metabolism and toxicity. In the former, we investigate the effects of bioreactor scale (7–5,000 L) and the addition of dextran sulfate, a commonly used anti-apoptotic agent (Dee et al. 1997; Zanghi et al. 2000), on the growth media and intracellular metabolome in CHO cells expressing a recombinant protein. Also, for the purpose of accurate quantification of low level components, we demonstrate that iteratively calculating and fitting the whole NMR spectrum by means of the quantum mechanical total line shape algorithm, produced the most accurate results, especially in the presence of challenging spectral overlap. In the rat liver slice model, we analyze the media for potentially growth-limiting nutrients.

Materials and methods

CHO cell experiments

The CHO cell line expressing a recombinant fusion protein used in these studies was subcloned from DG44 parental cells. Two cell culture processes are described; the first one, Process A, is utilized in the scale up study, a modified Process B, is utilized for the lab scale investigation of the effects of dextran sulfate addition. Both processes used the same cell line, but differed mainly in formulations for the proprietary serum-free growth, production, and feed media.

Bioreactor experiments were performed in 7-L (Sartorius, Goettingen, Germany) bioreactors with working volumes of approximately 4–6 L. Process A was also performed at large scale in 5,000-L bioreactors. Temperature was initially controlled at 37°C, but was shifted to a lower value during the culture to extend culture duration. For each experiment, the timing and magnitude of the temperature shift was the same for each bioreactor. The bioreactor pH was controlled by CO_2 gas and base addition. In addition to media formulations, the two processes differed with respect to determination of feed media volume and timing of addition of dextran sulfate, an additive found to inhibit apoptosis. The bioreactors were operated in fed-batch mode in which the feed volume was determined based upon the measured glucose concentration for Process A, but was fed using fixed volumes for Process B. The concentration of an additive found to inhibit apoptosis, dextran sulfate, was the same for both processes, but it was added when culture viability decreased below approximately 90% for Process A, or on day 3 for Process B. Viable cell density and percent viability were measured using automated cell counters. Culture samples were analyzed offline using a BioProfile 400 Analyzer to monitor pH, pCO_2, pO_2, glucose, glutamine, lactate, and ammonium (Nova Biomedical, Waltham, MA). Samples were pulled at various time points during the processes, and supernatants were prepared by centrifugation. In cases where cell extracts were analyzed, cell pellets containing an equal amounts of cells were washed twice

with 1× PBS and then frozen at −70°C prior to extraction as described below.

Liver slice experiments

Krebs-Henseleit buffer, Insulin (from bovine pancreas), Gentamicin, calcium chloride, glucose, sodium bicarbonate, HEPES were purchased from Sigma–Aldrich (St. Louis, MO). Waymouth MB752/1 was purchased from Invitrogen (Carlsbad, CA). Fetal bovine serum and Amphotericin-B were purchased from MediaTech, Inc. (Manasass, VA). Choline chloride was purchased from Fluka Analytical. L-Histidine was purchased from Alfa Aesar (a Johnson Matthey company). Acetonitrile (HPLC-grade) was obtained from Burdick and Jackson (Muskegon, MI). Formic acid (analytical-grade) was from J. T. Baker (Phillipsburg, NJ). All other reagents were of analytical grade. Lysing Matrix D Tubes were purchased from MP Biomedical (Solon, OH).

Male Sprague–Dawley rats (325–450 g, 10–15 weeks old, obtained from Charles River Laboratories, Raleigh, NC) were individually housed in a temperature- and light-controlled room. They were fed standard diet and water ad libitum. On the morning of each experiment rats were anesthetized with CO_2 and exsanguinated prior to hepatectomy and dissection of the liver into individual lobes, which were placed into ice-cold culture medium. Slices were prepared the day of each experiment using a protocol closely following previously published procedures (Lerche-Langrand and Toutain 2000; Olinga et al. 2001). Tissue cores were prepared with an 8 mm diameter motor-driven tissue coring tool (Alabama Research and Development Corporation, Munford, AL). Tissue slices, approximately 250 μm thick, were prepared in ice-cold culture medium using a Krumdieck tissue slicer (Alabama Research and Development Corporation, Munford, AL). Liver slice thickness was determined by macroscopic comparison to a 250 μm thickness gauge.

The slices were placed onto Vitron (Vitron Inc, Tucson, AZ) type C titanium roller inserts and cultured in glass scintillation vials containing 1.75 mL culture medium and continuously exposed to Carbogen (95% O_2/5% CO_2). The culture medium consisted of Waymouth's media supplemented with 25 mM HEPES, 10% fetal bovine serum, 5 μg/mL insulin, 50 μg/mL gentamicin, 2.5 μg/mL amphotericin B, 25 mM glucose, 2.4 g/L sodium bicarbonate with the final pH adjusted to 7.4. In one experiment, slices were incubated with the above culture medium for 0, 7 and 20 h and aliquots of media from those samples were removed periodically and stored at −80°C for non-targeted metabolomics analysis (see below). In a separate experiment to investigate the effect of choline and histidine augmentation, the above culture medium was modified by adding choline chloride (250 mg/L) and/or L-histidine (128 mg/L). Aliquots of 10 μL were taken from the media every 24 h (up to 94 h) to measure extracellular LDH activity as described below. After 94 h of incubation, slices and media were separated to facilitate slice processing for biochemical analysis. The slices were homogenized in 1 mL of 0.1 M phosphate buffer, pH 7.4 using Lysing Matrix D Tubes in the Savant FastPrep 120 (MP Biomedical, Solon, OH) shaker for 20 s. Liver slice supernatants were then obtained by centrifugation at approximately 5,000×g, for 5 min. Aliquots of the supernatant were used for lactate dehydrogenase (LDH), reduced glutathione (GSH) and adenosine triphosphate (ATP) measurements as described below. In a separate experiment, freshly prepared slices were processed as described above to obtain reference values of total intracellular GSH, ATP and LDH.

GSH, ATP and LDH measurements

Intracellular GSH was measured using a standard dithiobisnitrobenzoic acid (DTNB; Ellman's Reagent) assay. Slice homogenates were prepared as described above. Fifty μL of liver slice supernatant was added to 200 μL of a DTNB (3.96 mg/mL) solution in 0.1 M TRIS, pH 8.9. Absorbance at 405 nm was measured in a 96-well plate on a SpectroMax Pro spectrophotometer using SoftMax Pro software. GSH in slice homogenates were quantitated using a GSH standard curve from 25 to 250 μM.

Intracellular ATP was measured using a CellTiter-Glo Luminescent cell viability assay kit from Promega. Assay reagents were prepared according to the manufacturer. Immediately after slice processing, 100 μL of slice extract was combined with 100 μL of 10% trichloroacetic acid to stabilize the ATP. Ten μL of each sample were added to 100 μL of above assay reagent in a 96-well plate. The plate was incubated at room temperature for 30 min and read on a TopCount (Perkin Elmer) in luminescence mode.

Both extracellular and intracellular LDH were measured using a Raichem LDH assay kit according to the manufacturer. Ten μL of each sample (incubation media or liver slice extract) were added to 200 μL of the assay reagent in a 96-well plate. Data was captured on a SpectraMax plate reader using SoftMax Pro software in the kinetic setting.

NMR sample preparation

For CHO cell media measurements, samples were centrifuged to remove cells. For the investigation of scalability effects (process A), 0.4 mL of supernatants were mixed with 0.2 mL of 99.9% D_2O with 0.1 mM 1,1,2,2-tetradeutero-3-trimethylsilylpropionic acid (TSP) for reference. For experiments investigating the effect of dextran sulfate addition, (process B), 0.40 mL aliquots of the supernatant

were mixed with 0.20 mL of 0.2 M phosphate buffer in 20% D_2O, pH 7.0 (meter reading uncorrected for deuterium isotope effect) containing 0.1 mM TSP for reference. The samples were transferred to 5 mm NMR tubes and immediately queued up in the sample changer. Samples were maintained at 4–6°C until acquisition of spectra, which were collected at 27°C.

For CHO cell extracts, 1.0×10^7 cells frozen pelleted cells were mixed with 6 × volumes of dry ice-cold methanol in 2 mL eppendorf microfuge tubes, and a 3 mm carbide bead (Qiagen Inc., Valencia, CA) was added. The samples were subject to bead mill homogenization for 2 min at 30 Hz in a Retsch Model MM300 (Haan Germany) homogenizer. The extracts were centrifuged in an Eppendorf microfuge for 10 min at 4°C, 6,000 rpm, 0.5 mL of supernatant removed, and subjected to extraction by addition of 1 part of deionized water and two parts of chloroform. Samples were vortexed and centrifuged at 1,000 rpm for 1 h to aid phase separation. The water/methanol phase (top layer) was collected and dried under nitrogen flow overnight to remove all traces of solvent. Dried extracts were kept at −80°C until they were analyzed. For the scalability study (process A), samples were dissolved in 99.9% D_2O with 0.1 mM TSP; for the dextran sulfate addition study (process B), the extracts were dissolved with two parts of D_2O and one part of deuterated 0.2 M phosphate buffer as described above for supernatants, for a total volume of 0.6 ml. Once prepared, samples were transferred to 5 mm NMR tubes for NMR spectroscopy and immediately queued up in the sample changer. Samples were maintained at 4–6°C on the sample changer.

For liver slice experiments, 180 μL of media was mixed with 20 μL of a D_2O solution of 0.65 mg/mL of 1,1,2,2,3,3-hexadeutero-3-pentane sulfonic acid (DSS-d6) plus 0.21 mg/mL of 1,1-difluoro-1-trimethylsilanylmethylphosphonic acid (DFTMP) as an internal pH reference (Reily et al. 2006). Samples were placed into 3 mm NMR tubes and immediately placed into the NMR sample changer, where they were maintained at room temperature until analysis.

NMR spectroscopy

For CHO cell samples, 1D proton NMR spectra of supernatants and cell extracts were measured on a 600 MHz NMR Bruker spectrometer (Bruker Analytik, Rheinstetten, Germany) equipped with a 5 mm TCI cryoprobe and a SampleJet sample changer. Samples were maintained at 4–6°C while in the sample changer and then warmed to 27°C for measurement. A constant number of scans (256 for supernatants and 512 for cell extracts) and receiver gain were used into facilitate comparisons of relative analyte concentrations between samples. The pulse sequence used was a 1D version of a NOESY experiment with gradient water suppression during nOe mixing time of 0.05 s and during a relaxation time of 2 s. The 90° pulse width was automatically determined for each sample. All free induction decays (FID's) were subjected to Fourier transformation and automatic phase and baseline correction prior to calibrating to TSP at 0 ppm.

For liver slice media samples, 1D proton NMR spectra were measured on a 700 MHz NMR Bruker spectrometer (Bruker Analytik, Rheinstetten, Germany) equipped with a 5 mm TCI cryoprobe and a BACS-120 sample changer. A total of 256 transients digitized into 16K complex points were accumulated for each sample, with all inter-sample parameters held constant to facilitate comparisons of relative analyte concentrations between samples. The 90° pulse width was determined for the first sample. The pulse sequence used was a 1D version of a NOESY experiment with continuous wave saturation of the water signal during the nOe mixing time of 0.10 s and during a relaxation time of 2.4 s. All FID's were subjected to Fourier transformation, and manual phase and baseline-correction prior to calibrating to DSS at 0 ppm.

Data analysis and quantification of metabolites

For CHO cell analysis, a quantum mechanical total-line-shape fitting (QMTLS) approach was used to quantify up to 32 metabolites in two separate models for either supernatant or extract built from the metabolite database bbiorefcode-2-0-0 (Bruker BioSpin, Rheinstetten, Germany). The QMTLS models provide starting values for chemical shifts, proton-proton couplings, individual line widths for each spin-particle and the individual metabolite populations, which were then iteratively optimized to fit the experimental data for each data set in an automated batch-run using PERCH NMR Software (PERCH Solutions Ltd., Kuopio, Finland). Both integral transform and total-line-shape fitting were used in two subsequent steps (Laatikainen et al. 1996) first adjusting smaller variations of chemical shifts up to several Hz, and then also optimizing coupling constants, individual line-widths and the line-shape (Gaussian/Lorentzian contribution) for each spin-particle, followed by a baseline optimization routine using a mixture of Fourier and polynomial terms. The relative metabolite populations were normalized to the sum of all integrals in each spectrum. No attempt was made to normalize to total signal intensity due to dissimilar protein signal background in the spectra. The data analysis and visualization was performed utilizing the Partek Genomics Suite package (Version 6.5, Partek Inc. St Louis, Missouri).

For analysis of the liver slice media and for some measurements of CHO cell media components, spectra were integrated in the program AMIX version 3.9 (Bruker

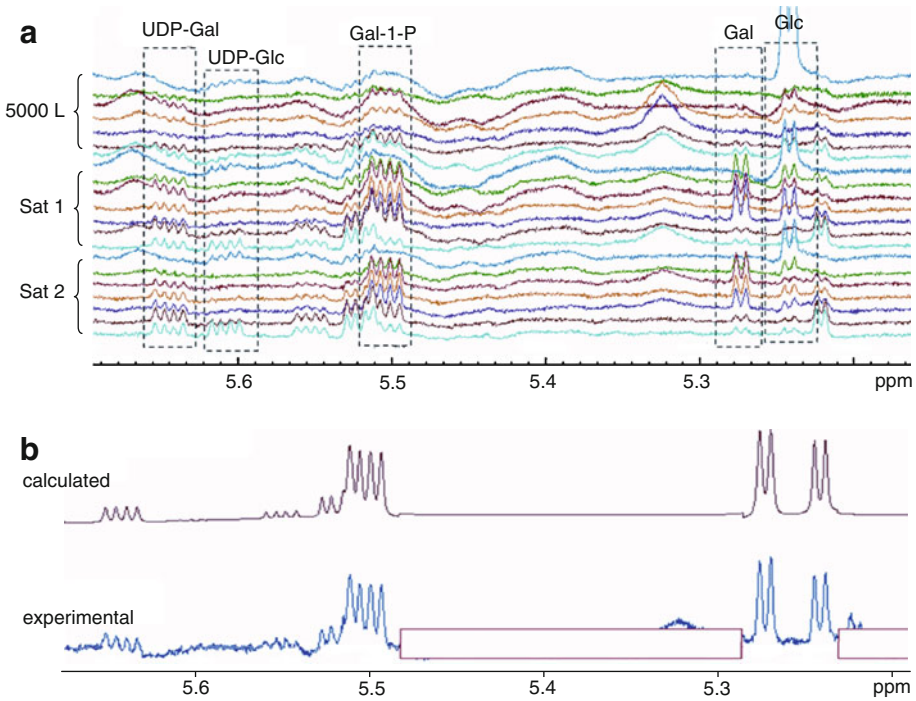

Fig. 1 Phosphoglycoside NMR spectral region for cell extracts, showing low signal to noise and base line artifacts which cannot be accurately corrected by a spline function. **a** experimental data showing annotated regions of interest. **b** Quantum mechanic total line shape fitting of the same region for a single spectrum of CHO cell extract. The *rectangles* over the baseline in the experimental trace in **b** indicate spectral regions that were explicitly omitted from the calculations

BioSpin, Rheinstetten, Germany) using the "multi-integrate" routine and defining integration regions around selected peaks interactively while observing all spectra superimposed or stacked vertically to ensure proper inclusion of the peak of interest and exclusion of extraneous peaks across the entire dataset—essentially a visually guided bucketing approach. The output from AMIX was exported to Microsoft Excel for statistical analysis and evaluation. One drawback to this method is that, even for reasonably well pronounced peaks, the baseline in such samples is rarely totally devoid of intensity due to non-zero baseline or low level overlapping peaks. Therefore, even in the total absence of a particular target component, a non-zero integral may be obtained.

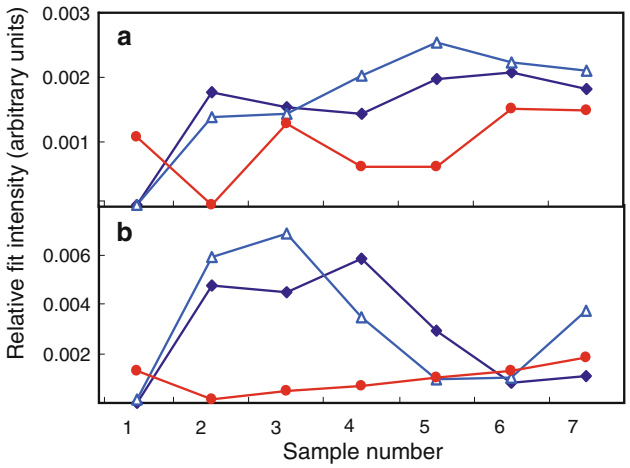

Fig. 2 Time course of relative intracellular concentrations of galactose (*bottom*) and its activated form, galactose-UPP (*top*) in the large (*red circles*) and satellite 1 (*dark blue diamonds*) and satellite 2 (*light blue triangles*) experiments over the course of a 10 day culture. Sample numbers correspond to: 1—day of inoculation; 2—day 5 before addition of dextran sulfate; 3—day 5 after addition of dextran sulfate; 4—day 6 before temperature shift; 5—day 6 after temperature shift; 6—day 8; 7—day 10

Results and discussion

Effect of scale on CHO cell production

For this scalability study, a 1 h post-inoculation aliquot of a production size (5,000 L) bioreactor was obtained for inoculation of two lab-scale bioreactors (7 L, satellites 1 and 2). All three systems were nourished with identical feed medium and kept at otherwise constant fermentation parameters (temperature, pH, etc.). Supernatants and cell pellets were collected as described above. Metabolite concentrations measured by NMR for all three samples were compared directly to each other, since there was some variability between both satellites and not enough power for statistical analysis (N = 2 for satellites and N = 1 for 5,000 L). It is not uncommon to observe a decrease in productivity upon scale-up in recombinant protein expression (Hu and Aunins 1997). Indeed, in this study, the 7 L batches presented higher viability at the end of the culture (83% vs. 65%) and productivity (up to twofold more

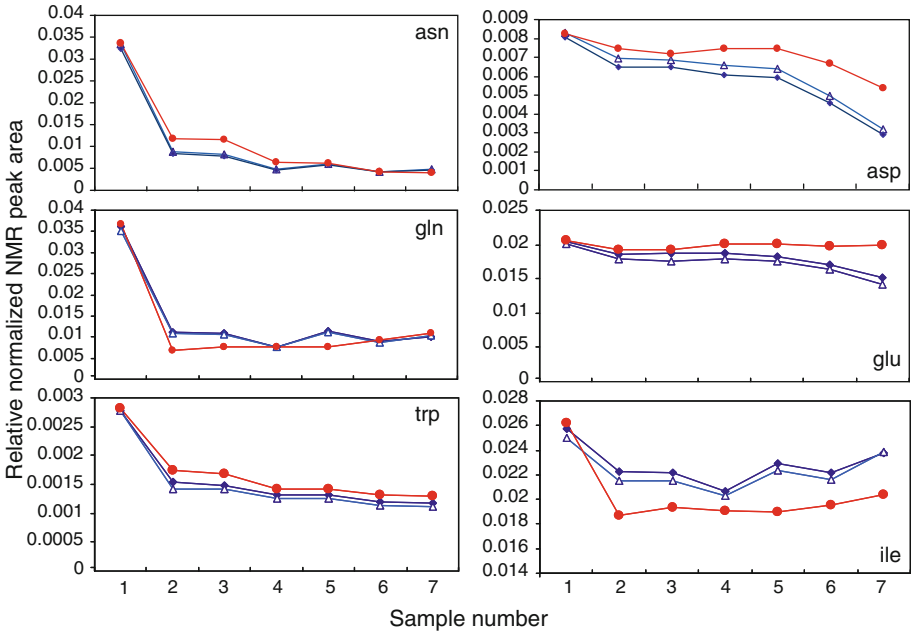

Fig. 3 Time course of relative selected extracellular amino acid concentrations in the in the large (*red circles*) and satellite 1 (*dark blue diamonds*) and satellite 2 (*light blue triangles*) experiments over the course of a 10 day culture. Sample numbers correspond to: 1—day of inoculation; 2—day 5 before addition of dextran sulfate; 3—day 5 after addition of dextran sulfate; 4—day 6 before temperature shift; 5—day 6 after temperature shift; 6—day 8; 7—day 10

protein per unit volume) under otherwise identically controlled conditions. In order to elucidate possible biochemical mechanisms that would account for this phenomenon, a comparison of the metabolomics data from media supernatants from the three bioreactors was carried out.

The cell extracts and supernatants showed many differences in the metabolites that were detectable and measurable. The most striking differences were in the energy-activated molecules such as adenosine nucleoside phosphates (AXPs), and activated glycosides such as UDP-glucose, 1,6-glucose bisphosphate (Glu-PP), UDP-galactose, etc., which were only detectable in the cell extracts, and certain tricarboxylic acid metabolites including citric and 2-oxoglutaric acids, which were only found in the supernatants.

The intracellular metabolites that discriminated most between the production batch and the small scale satellites included the activated glycosides and sugars. The signals of the sugar phosphates and sugars were close to the water signal where some suppression artifacts distorted the baseline, and were of very small intensity. Under such conditions, the advantage of the QMTLS approach for measuring some of these very low level metabolites becomes apparent and is illustrated in Fig. 1. The activated glycosides increased steadily with time in the satellite batches, but apparently to a lesser extent in the large scale batch, Fig. 2a. On the other hand galactose, which is part of the daily feed, disappears quickly from the media in the large batch extracts as evidenced by its consistently low level, while it was present at higher levels through day 4 in both the satellite batches, as shown in Fig. 2b.

In the supernatants, the metabolites that differentiated scale were Asn/Asp and Glu/Gln pairs, and aromatic and branched chain amino acids, Fig. 3. The rate of glucose and galactose depletion was faster in the 5,000 L bioreactor, while more citrate and other Krebs cycle intermediates were produced in the small bioreactor than in the production size one, as illustrated in Fig. 4 for galactose and citrate. Galactose is a fed component, so the lower levels in at each time point in the 5,000 L batch indicate more rapid utilization of this carbohydrate; glucose utilization shows a similar trend. Similarly, Krebs cycle intermediates, exemplified by citrate, are only produced by the cells (i.e. are not media or feed components) and these increase at later time points in the culture more significantly in the smaller bioreactors. Both of these observations point to a higher reliance of the cells in the large bioreactor on glycolysis for energy compared with those growing at the lab scale. It is known that galactose as carbon source prolongs cell viability, postpones onset of apoptosis and reduces lactate concentration in the medium (Altamirano et al. 2006). We observed that, in spite of increased utilization of glucose and galactose in the large batch, lactate levels remained comparable in the small and large batches up to day 6 post temperature shift, increasing only at the two final days 8 and 10, after complete galactose depletion, Fig. 4. Activated and phosphorylated galactose and other activated cofactors needed for the conversion of galactose to glucose via the Leloir pathway (Frey 1996) need ATP, which is produced mostly during the Krebs mitochondrial respiration cycle. Given our findings, it is tempting to hypothesize that in the large batch, cells are producing their energy mostly through anaerobic glycolysis, where galactose consumption allows for extended viability under suboptimal conditions. Thus, it may be that oxygen availability

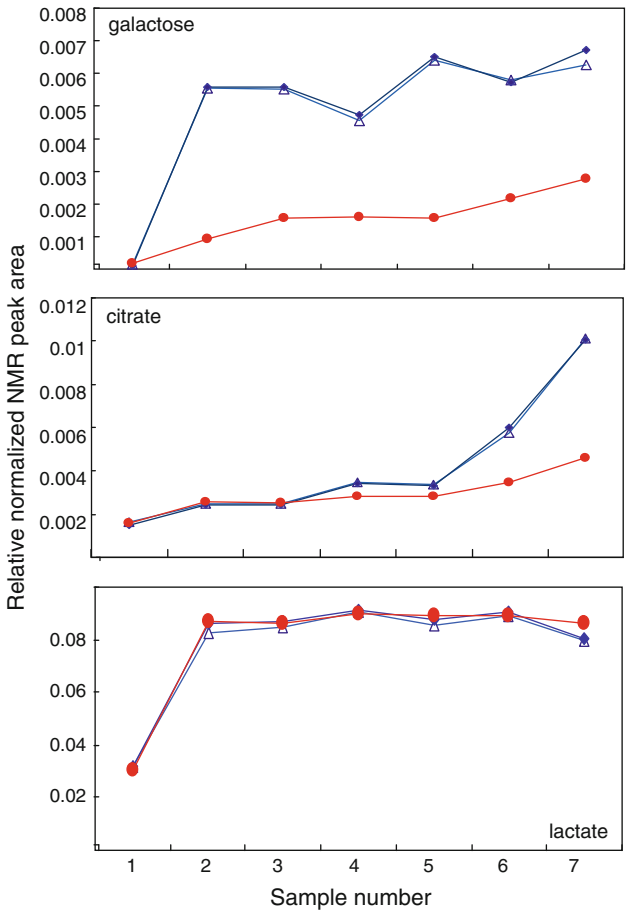

Fig. 4 Galactose utilization is higher in the large scale conditions (*red circles*), while citrate concentrations increase in the small batches (*blue triangles and diamonds*), and lactate levels remain constant over the course of a 10 day culture. Sample numbers correspond to: 1—day of inoculation; 2—day 5 before addition of dextran sulfate; 3—day 5 after addition of dextran sulfate; 4—day 6 before temperature shift; 5—day 6 after temperature shift; 6—day 8; 7—day 10

and consumption for all cells at all times during the process (micro aerobic conditions), which would allow for enhanced mitochondrial function and TCA cycle activity, may not be optimally achieved in production size batch, as compared to laboratory scale batches.

Effect of dextran sulfate on CHO cell production

In order to elucidate possible biochemical mechanisms of the empirically observed titer-enhancing effect of added dextran sulfate (DS), six lab-scale (7 L) bioreactors were run concurrently, 3 with and 3 without DS. Samples were collected at several times during the entire 14 day culture period.

Most of the significant differences in metabolic profiles in the supernatants from all six reactors were in the time coordinate, with the major changes being the depletion of Asn and Asp from the medium by days 4, and 7 respectively, and glycerol accumulating after day 6. Regions of the daily spectra from all bioreactor samples with and without dextran sulfate added are shown superimposed in Fig. 5. Glucose changes were also quantified, but because this nutrient was given as an ad hoc bolus when levels dropped below a certain threshold, the measurements were not correlated to any of the variables, time or treatment. The metabolites in the supernatants showed different concentration trends depending upon the metabolite; since we were interested in metabolic trajectories that would distinguish between cultures with and without DS, the findings can be grouped into three categories as follows: metabolites that behave identically with or without DS (e.g. asparagine, aspartic acid), metabolites that differentially accumulate with DS (e.g. uracil, niacinamide, some essential amino acids, acetate, fumaric acid, lactate, sugars other than galactose and glucose), and metabolites that express differently during the temperature shifts (e.g. AXP, citrate, valine, alanine). The temporal change in concentration of representatives of each of these categories is illustrated in Fig. 6 and is comprehensively summarized in Table 1.

It has been empirically demonstrated that during the temperature shift CHO cells rearrange their biosynthetic machinery to arrest cell division and growth and increase

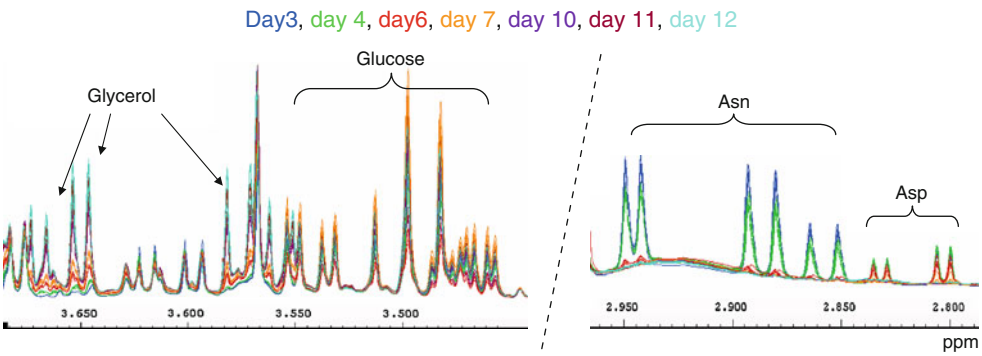

Fig. 5 NMR spectra showing changes of extracellular metabolites from a single culture containing dextran sulfate with time include utilization of carbon (glucose, glycerol) and nitrogen sources (e.g. asparagine). Spectra are color coded by day

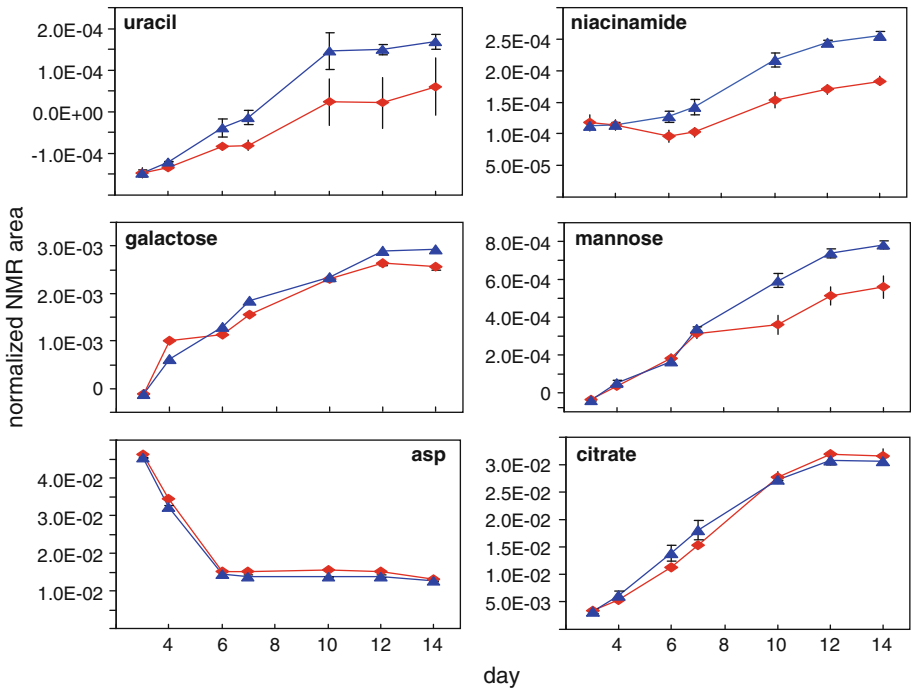

Fig. 6 Time course of selected extracellular metabolite relative concentrations with (*blue triangles*) and without (*red diamonds*) dextran sulfate over the course of a 14 day culture. *Error bars* indicate 1 standard deviation from the mean (N = 3)

Table 1 Metabolite changes in media with and without dextran sulfate

Metabolite	Percent difference[a]	Metabolite	Percent difference[a]
MNNA	−11.7	Serine	−2.6
Niacinamide	39.1	Lysine	−4.8
Histidine	−3.0	Asparagine	−3.9
Tryptophane	−11.2	Aspartic acid	−5.1
Phenylalanine	−4.5	Methionine	−2.0
Tyrosine	−14.8	Citrate	−3.1
Fumaric acid	−16.2	Pyroglutamate	8.2
Uracil	64.3	Valine	−9.8
Galactose	12.5	Glutamate	1.2
Glucose	17.5	Acetate	23.6
4-Hydroxyproline	−4.1	Butyrate	−18.2
Malic acid	−8.9	Alanine	4.5
Threonine	−7.4	Lactate	−0.2
Asparagine	−0.4	Isoleucine	−7.5

[a] Percent difference is: (100 × (A − B))/(A + B), where A the sum of peak areas from all time points the DS supplemented media and B the sum of peak areas from all time points of the unsupplemented media

protein synthesis (Moore et al. 1997). Changes in metabolites during the temperature shift that are related to energy utilization, such as citrate, acetate, alanine and AXP, may indicate a change in energy utilization optimized for protein synthesis. Furthermore, we observed DS-induced changes in nucleotide concentrations, which may indicate changes in their utilization and biosynthesis. For example, uracil and niacinamide begin to enrich 24 h after DS addition and days before the temperature shift. This suggests that dextran sulfate both improves viability and growth during the cell growth period, and enhances energy utilization post temperature shift, when protein synthesis is emphasized. Interestingly, these observations correspond temporally with experimentally determined cellular aggregation, which showed that the level of aggregation was significantly lower in the DS-treated batches starting after about day 5 and through the end of the culture, Fig. 7a. Cell viability and productivity also correlated with many of the metabolite measurements. The viability of the cells started differentiating significantly at day 8 (difference of 1.6%) and the difference kept increasing until the end of the process (difference of 5.5%) even though the total number of cells in all batches was not significantly different, Fig. 7b. The titer, a direct measure of the protein production, started differentiating at day 6 and continued increasing until the harvest, Fig. 7c. Thus, the phenomenon of cell aggregation and the observed cell viability and titer are all temporally correlated to the metabolomic changes described above.

Liver slice metabolomics

The precision-cut liver slice is a commonly used model for assessing drug metabolism and certain types of hepatotoxicities in vitro (Laskin and Pilaro 1986; Laskin et al. 1986; Goldin et al. 1996). The recipe for this model is well established (Lerche-Langrand and Toutain 2000) and relies on commercially available media and common additives

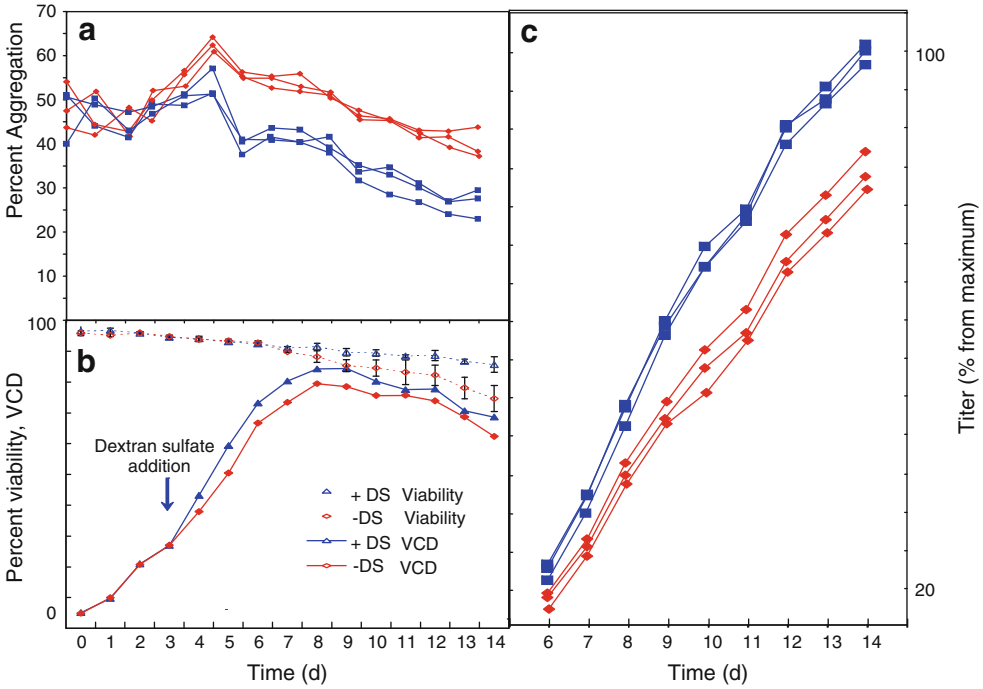

Fig. 7 Time course of various commonly measured culture parameters for lab scale bioreactions with (*blue*) and without (*red*) dextran sulfate. **a** Percent cell aggregation, individual bioreactor readout; **b** percent viability and viable cell density (VCD), mean readouts for each group ± standard deviation; **c** percent titer (from maximum), individual bioreactor readout

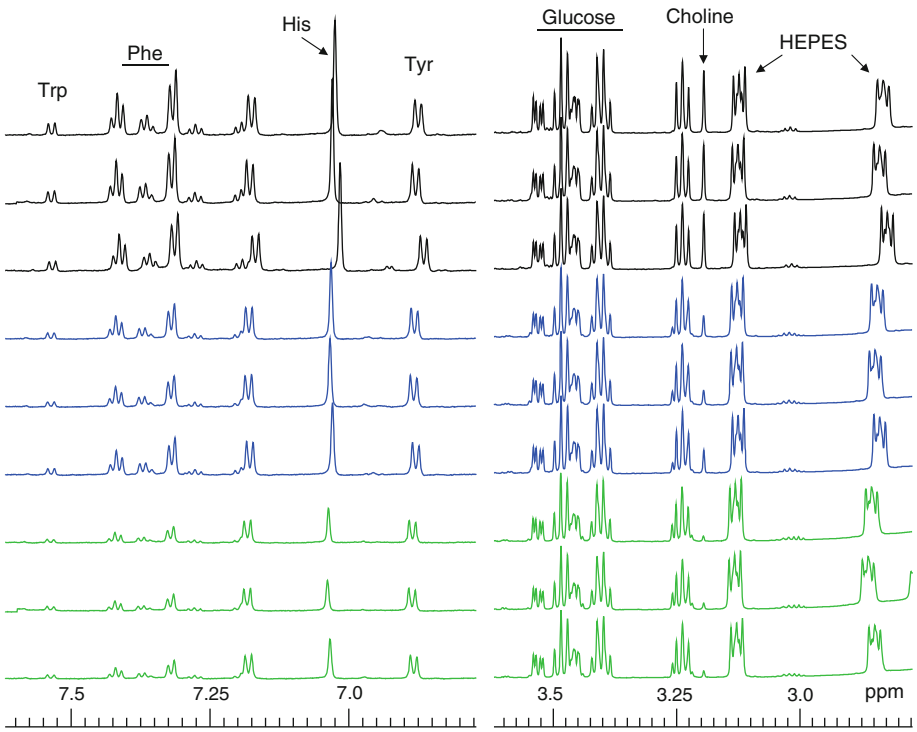

Fig. 8 Selected regions of the 700 MHz 1H NMR spectrum of liver slice (Waymouth's) media over a 20 h culture. Spectra were acquired on biological triplets at 0 (*black*), 7 (*blue*) and 20 (*green*) hours of incubation. All slices came from a single rat. Selected components are labeled

(see "Materials and methods"). In practice, liver slices can typically be maintained in a healthy state for at least 20 h without changing media in this model. We were interested in applying metabolomic technology to study the changes in culture media as a function of culture duration and viability. With a complete knowledge of the makeup of the media, it was possible to quantitatively assess the disappearance of nutrients and appearance of metabolites produced by the liver slices themselves. Figure 8 shows selected regions of NMR spectra obtained on media at various times of incubation up to 20 h. As can be seen, several components such as choline, histidine and tryptophan are dramatically reduced in concentration, whereas others, such as alanine, 3-hydroxybutyrate (BHB) and lactate increase over time. Mean relative levels of some of these are shown in Fig. 9. Since lactate was speculated to

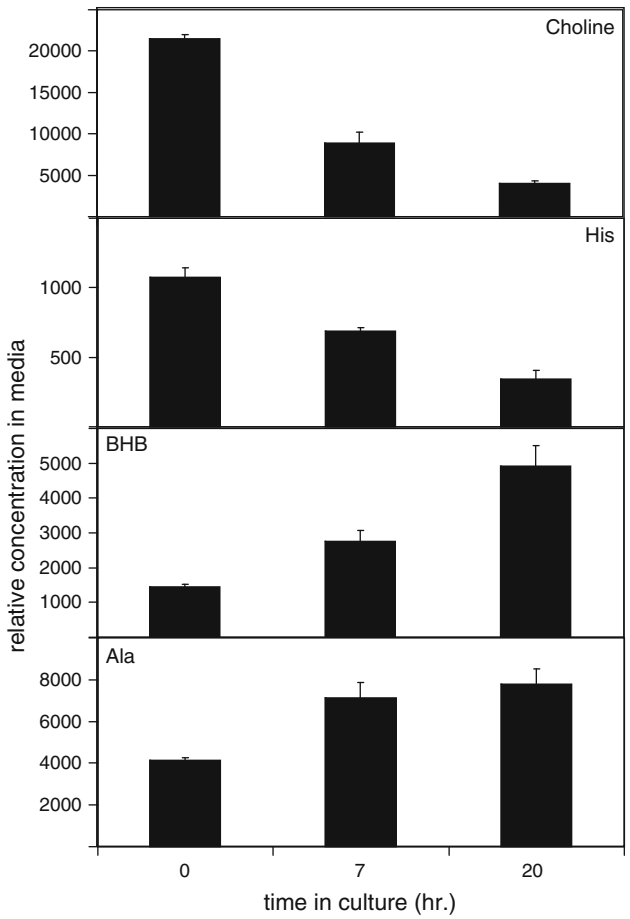

Fig. 9 Changes in relative concentration (arbitrary NMR intensity units) of selected metabolites in the media throughout the course of the liver slice culture. Choline and histidine are provided nutrients in the media and are depleted, whereas Ala and 3-hydroxybutyric acid (BHB) are products of the liver slice metabolism. *Error bars* indicate 1 standard deviation from the mean (N = 3)

arise from glycolysis within the liver slices, glucose and lactate were also measured, and a clear relationship between lactate production in the tissue and depletion of supplied glucose is observed, Fig. 10. It should be pointed out that although alanine, lactate and BHB are not present in the media itself, integrated intensity is non-zero at T = 0, because of the binning method used to quantify in this part of the work. Although QMTLS would have provided superior results, it was not available at the time this work was done. Nonetheless, as can be seen by the standard deviations in the data (N = 3) in Fig. 9 and 10, the biological variation was extremely small and the changes in these metabolites are very clear.

Based on the apparent depletion of certain metabolites around the time the slices tend to begin to fail, histidine and choline in particular, we speculated that these compounds may be essential for viability. To test this hypothesis, we augmented the culture media with a twofold excess of each of these metabolites individually and together and

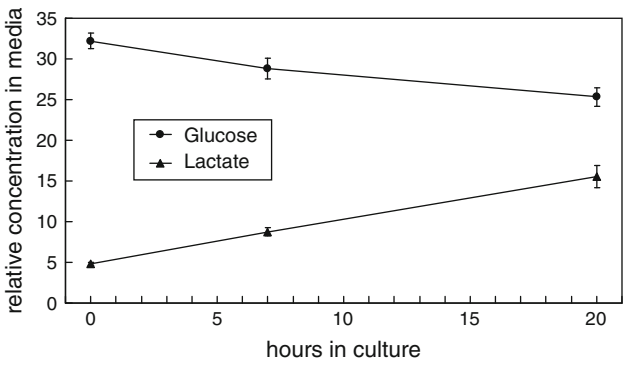

Fig. 10 Changes in the relative concentrations of glucose and lactate over the 20 h incubation as measured by the anomeric proton of glucose and methine proton of lactate. *Error bars* indicate 1 standard deviation from the mean (N = 3)

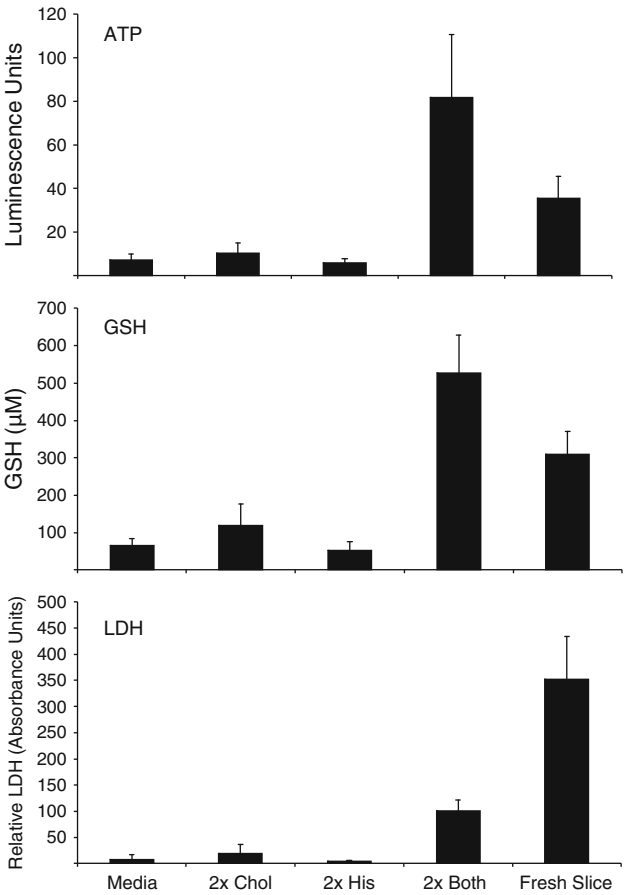

Fig. 11 Tissues levels of LDH, GSH and ATP and at the end of a 94-h experiment in normal and augmented media. The bar at the far right is a reference level taken from a different liver immediately after slice preparation, and is simply provided as a reference for approximate levels in fresh tissue. *Error bars* indicate 1 standard deviation from the mean (N = 3)

measured cell viability parameters, such as GSH, ATP and LDH in the liver slices. Higher levels of these in the tissue are consistent with viable tissue. Even after 94 h, when

both His and choline are increased, the levels of these markers of cellular function are close to levels found in fresh liver slices, whereas they are significantly depleted with normal media or media augmented with His or choline alone, Fig. 11. These results indicate that, even at the very long incubation times the cells seem more viable when augmented with both limiting metabolites.

Conclusions

We have demonstrated that NMR-based metabolomics is useful for simultaneous monitoring of many supplied and excreted small molecules in living mammalian cells. Unlike conventional biochemical analysis, a metabolomics approach allows the quantification of many metabolites of which could not be anticipated to be significant a priori. With this information, we can probe the health and viability of mammalian cell or tissue cultures and identify which small molecule media components may affect cell growth and viability. This can either be by the early depletion of an essential nutrient or by excessive build-up of metabolites deleterious to the cell. Further, we can generate hypotheses that, once tested, can provide insight to biochemical mechanisms. This application of metabolomics avoids many of the pitfalls of studying whole animals, since there are fewer concurrent processes and nutrient influx and efflux can be more closely controlled and measured. In a protein production setting, metabolomics can dramatically increase the information available on the on biochemical changes occurring within the culture, since relatively few selected metabolites and parameters are traditionally monitored. Here, we have shown its utility in discovering previously unknown molecular modulations induced by physical (reactor size) and chemical (dextran sulfate) perturbations in engineered CHO cells. Similarly, in a widely used tissue culture model, we have shown that metabolomics can identify critical supplied nutrients that can potentially extend the culture duration of the model and therefore it's usefulness. Finally we have demonstrated that by considering each metabolite as a complete spin system that must obey certain quantum mechanical rules, we can provide highly accurate relative metabolite concentrations even for low level metabolites in the presence of strong overlap, higher order effects, severe baseline distortion and background interference.

References

Adams MA, Chen Z, Landman P, Colmer TD (1999) Simultaneous determination by capillary gas chromatography of organic acids, sugars, and sugar alcohols in plant tissue extracts as their trimethylsilyl derivatives. Anal Biochem 266:77–84

Altamirano C, Illanes A, Becerra S, Cairo JJ, Godia F (2006) Considerations on the lactate consumption by CHO cells in the presence of galactose. J Biotechnol 125:547–556

Bradley SA, Ouyang A, Purdie J, Smitka TA, Wang T, Kaerner A (2010) Fermentanomics: monitoring mammalian cell cultures with NMR spectroscopy. J Am Chem Soc 132:9531–9533

Chong WPK, Goh LT, Reddy SG, Yusufi FNK, Lee DY, Wong NSC, Heng CK, Yap MGS, Ho YS (2009) Metabolomics profiling of extracellular metabolites in recombinant Chinese Hamster ovary fed-batch culture. Rapid Commun Mass Spectrom 23:3763–3771

Chong WPK, Reddy SG, Yusufi FNK, Lee DY, Wong NSC, Heng CK, Yap MGS, Ho YS (2010) Metabolomics-driven approach for the improvement of Chinese hamster ovary cell growth: overexpression of malate dehydrogenase II. J Biotechnol 147:116–121

Chrysanthopoulos PK, Goudar CT, Klapa MI (2010) Metabolomics for high-resolution monitoring of the cellular physiological state in cell culture engineering. Metab Eng 12:212–222

Cuperlovic-Culf M, Barnett DA, Culf AS, Chute I (2010) Cell culture metabolomics: applications and future directions. Drug Discov Tod 15:610–621

Dee KU, Shuler ML, Wood HA (1997) Inducing single-cell suspension of BTI-TN5B1–4 insect cells: I. The use of sulfated polyanions to prevent cell aggregation and enhance recombinant protein production. Biotechnol Bioeng 54:191–205

Dunn WB, Brown M, Worton SA, Crocker IP, Broadhurst D, Horgan R, Kenny LC, Baker PN, Kell DB, Heazell AEP (2009) Changes in the metabolic footprint of placental explant-conditioned culture medium identifies metabolic disturbances related to hypoxia and pre-eclampsia. Placenta 30:974–980

Frey PA (1996) The Leloir pathway: a mechanistic imperative for three enzymes to change the stereochemical configuration of a single carbon in galactose. FASEB J 10:461–470

Goldin RD, Ratnayaka ID, Breach CS, Brown IN, Wickramasinghe SN (1996) Role of macrophages in acetaminophen (paracetamol)-induced hepatotoxicity. J Pathol 179:432–435

Gomez-Lechon MJ, Lahoz A, Gombau L, Castell JV, Donato MT (2010) In Vitro evaluation of potential hepatotoxicity induced by drugs. Curr Pharm Des 16:1963–1977

Hu W-S, Aunins JG (1997) Large-scale mammalian cell culture. Curr Opin Biotechnol 8:148–153

Issaq HJ, Van QN, Waybright TJ, Muschik GM, Veenstra TD (2009) Analytical and statistical approaches to metabolomics research. J Sep Sci 32:2183–2199

Jellum E, Kvittingen EA, Stokke O (1988) Mass spectrometry in diagnosis of metabolic disorders. Biomed Environ Mass Spectrom 16:57–62

Laatikainen R, Niemitz M, Weber U, Sundelin J, Hassinen T, Vepsäläinen J (1996) General Strategies for total-lineshape-type spectral analysis of NMR spectra using integral-transform iterator. J Magn Reson Ser A 120:1–10

Laskin DL, Pilaro AM (1986) Potential role of activated macrophages in acetaminophen hepatotoxicity. I. Isolation and characterization of activated macrophages from rat liver. Toxicol Appl Pharmacol 86:204–215

Laskin DL, Pilaro AM, Ji S (1986) Potential role of activated macrophages in acetaminophen hepatotoxicity. II. Mechanism of macrophage accumulation and activation. Toxicol Appl Pharmacol 86:216–226

Lerche-Langrand C, Toutain HJ (2000) Precision-cut liver slices: characteristics and use for in vitro pharmaco-toxicology. Toxicology 153:221–253

Lim Y, Wong NSC, Lee YY, Ku SCY, Wong DCF, Yap MGS (2010) Engineering mammalian cells in bioprocessing—current

achievements and future perspectives. Biotechnol Appl Biochem 55:175–189

Lindon JC, Nicholson JK, Everett JR (1999) NMR spectroscopy of biofluids. Ann Rep NMR Spect 38:1–88

Moore A, Mercer J, Dutina G, Donahue CJ, Bauer KD, Mather JP, Etcheverry T, Ryll T (1997) Effects of temperature shift on cell cycle, apoptosis and nucleotide pools in CHO cell batch cultures. Cytotechnology 23:47–54

Nicholson JK, Lindon JC, Holmes E (1999) 'Metabonomics': understanding the metabolic responses of living systems to pathophysiological stimuli via multivariate statistical analysis of biological NMR spectroscopic data. Review 28 refs. Xenobiotica 29:1181–1189

Olinga P, Merema MT, De Jager MH, Derks F, Melgert BN, Moshage H, Slooff MJH, Meijer DKF, Poelstra K, Groothuis GMM (2001) Rat liver slices as a tool to study LPS-induced inflammatory response in the liver. J Hepatol 35:187–194

Pauling L, Robinson AB, Teranishi R, Cary P (1971) Quantitative analysis of urine vapor and breath by gas-liquid partition chromatography. Proc Natl Acad Sci USA 68:2374–2376

Reily MD, Robosky LC, Manning ML, Butler A, Baker JD, Winters RT (2006) DFTMP, an NMR reagent for assessing the near-neutral pH of biological samples. J Am Chem Soc 128:12360–12361

Robertson DG, Reily MD, Baker JD (2007) Metabonomics in pharmaceutical discovery and development. J Proteome Res 6:526–539

Sauter H, Lauer M, Fritsch H (1991) Metabolic profiling of plants—a new diagnostic technique. ACS Symp Ser 443:288–299

Seagle C, Christie MA, Winnike JH, McClelland RE, Ludlow JW, O'Connell TM, Gamcsik MP, Macdonald JM (2008) High-throughput nuclear magnetic resonance metabolomic footprinting for tissue engineering. Tissue Eng Part C Methods 14:107–118

Trethewey RN, Krotzky AJ, Willmitzer L (1999) Commentary. Metabolic profiling: a Rosetta stone for genomics? Curr Opin Plant Biol 2:83–85

Zanghi JA, Renner WA, Bailey JE, Fussenegger M (2000) The growth factor inhibitor suramin reduces apoptosis and cell aggregation in protein-free CHO cell batch cultures. Biotechnol Prog 16:319–325